Journal of Advanced Research (2010) **1**, 129–136

Cairo University

Journal of Advanced Research

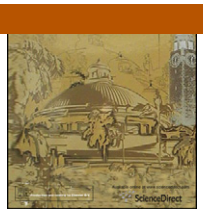

ORIGINAL ARTICLE

Effect of applying static electric field on the physical parameters and dynamics of laser-induced plasma

Asmaa Elhassan[a], **Hussein M. Abd Elmoniem**[b], **Arafa K. Kassem**[a], **Mohamed A. Hairth**[a,*]

[a] *National Institute of Laser Enhanced Sciences (NILES), Cairo University, Egypt*
[b] *Department of Physics, Faculty of Science, Cairo University, Egypt*

Available online 6 March 2010

KEYWORDS

Laser-induced plasma;
Static electric field;
Shock waves;
Plasma dynamics

Abstract In order to improve the performance of the LIBS technique – in particular its sensitivity, reproducibility and limit of detection – we studied the effect of applying a static electric field with different polarities on the emission spectra obtained in a typical LIBS set-up. The physical parameters of the laser-induced plasma, namely the electron density N_e and the plasma temperature T_e, were studied under such circumstances. In addition to the spectroscopic analysis of the plasma plume emission, the laser-induced shock waves were exploited to monitor the probable changes in the plasma plume dynamics due to the application of the electric field. The study showed a pronounced enhancement in the signal-to-noise (S/N) ratio of different Al, neutral and ionic lines under forward biasing voltage (negative target and positive electrode). On the other hand, a clear deterioration of the emission line intensities was observed under conditions of reversed polarity. This negative effect may be attributed to the reduction in electron-ion recombinations due to the stretched plasma plume. The plasma temperature showed a constant value in the average with the increasing electric field in both directions. This effect may be due to the fact that the measured values of T_e were averaged over the whole plasma emission volume. The electron density was observed to decrease slightly in the case of forward biasing while no significant effect was noticed in the case of reversed biasing. This slight decrease in N_e can be interpreted in view of the increase in the rate of electron–ion recombinations due to the presence of the electric field. No appreciable effects of the applied electric field on the plasma dynamics were noticed.

Introduction

Laser Induced Breakdown Spectroscopy (LIBS) is a simple analytical technique which has been utilised in the analysis of solid [1], liquid [2] and gaseous [3] samples. In the LIBS technique an intense laser pulse is focused onto a material target, and identification of the material's elemental composition can then be made by measuring lines of emission from ions and excited neutral atoms in a transient laser produced plasma. The great appeal of LIBS lies in the fact that little or no sample preparation is required to obtain useful results and the technique is readily portable to the field. The technique and its applications have been thoroughly discussed in a number of review books [4,5].

* Corresponding author. Tel.: +20 2 35675335; fax: +20 2 35675335.
E-mail address: mharithm@niles.edu.eg (M.A. Hairth).

doi:10.1016/j.jare.2010.03.004

Despite its advantages, the LIBS technique does, however, have a number of limitations, including self-absorption of emissions, line broadening, and continuum background [6]. These limitations may be minimised by optimal time gating. Another limitation is the sensitivity of the system. In this, the detection sensitivity of the system can be significantly enhanced through the optimisation of several critical parameters. Here the plasma production is influenced by laser parameters (intensity, pulse duration, and wavelength) [7–9], the physical properties of the target material (z-number, ionisation potential, reflectivity and thermal conductivity), and by the ambient conditions. There are several ways to improve the performance of LIBS. These include the use of multiple laser pulses [10,11], the introduction of buffer gas around the plasma [12] and the application of a magnetic field [13]. Since plasma is a high energy electrically charged mixture of ions and electrons, it is expected to respond to electric fields. By applying a static electric field on the laser-induced plasma, it is possible to produce more intense spectral lines and sustain the emission for longer periods of time. Here Hontzopoulos et al. [14] have reported that the laser plasma emission from a gold target in the ultraviolet spectral region was enhanced by more than one order of magnitude in the presence of a high negative static electric field. Their results suggest that the laser plasma creation in the presence of a high static electric field may provide a convenient method for the development of a high brightness, point like UV light source even at relatively low laser intensities.

The aim of the present work was to investigate the effect of applying a static electric field of relatively low strength on the laser-induced plasma parameters. Using an echelle spectrometer facilitated the study of a broad spectral range covering emission lines in the UV, visible and near-IR regions. The effect of the electric field on the plasma plume dynamics was studied by monitoring the laser-induced shock waves.

Methodology

Fig. 1 shows the schematic diagram of the experimental setup. Laser-induced plasma was obtained using a Q-switched Nd:YAG laser (Continuum NY81.30, USA) delivering laser pulses of 60 mJ/pulse, with pulse duration of 7 ns at its fundamental wavelength (1064 nm) with adjustable repetition rate up to 30 Hz. The laser pulse energy was adjusted by a suitable combination of beam splitters at constant operating high voltage (1.3 kV) and delay (1.5 μs) to ensure spatial and temporal beam profile stability. An energy meter (Nova, Ophir Optronics Ltd., USA) was employed to monitor the shot to shot laser pulse energy. The laser beam was focused onto the aluminium target surface via a quartz plano-convex lens of 50 mm focal length. The emission light from the plasma plume was collected using a telescopic optical system of two lenses (not shown in the figure). The collected light was fed to the free terminal of a one-meter length wide-band fused-silica optical fibre (600 μm) connected at its other end to an echelle spectrometer (Mechelle 7500, Multichannel Instruments, Sweden). This spectrometer provides a constant spectral resolution of 7500 corresponding to 4 pixels FWHM, over a wavelength range 200–1000 nm displayable in a single spectrum. A gateable, intensified CCD camera, (DiCAM-Pro, PCO Computer Optics, Germany) coupled to the spectrometer was used for detection of the dispersed plasma emission light. The overall linear dispersion of the spectrometer-camera system ranged from 0.006 nm/pixel (at 200 nm) to 0.033 nm/pixel (at 1000 nm). To avoid electronic interference and jitters, the CCD intensifier high voltage was triggered optically. Special Multichannel Instruments software

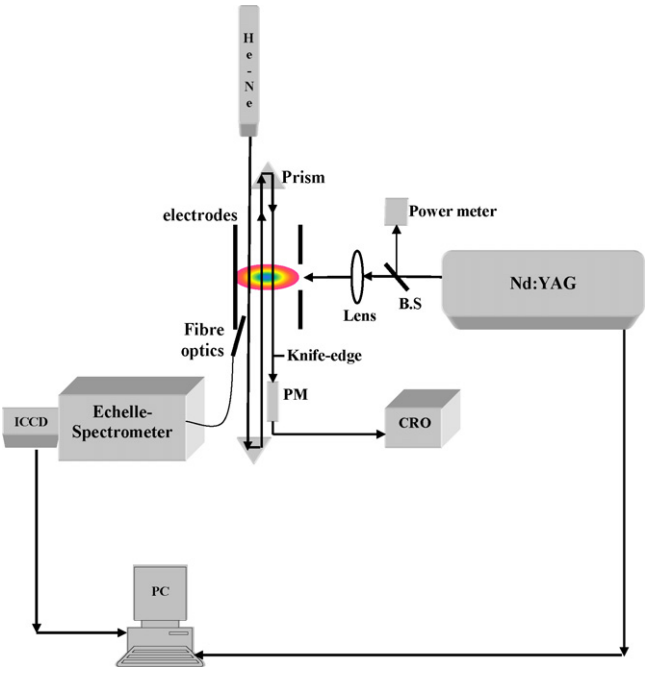

Figure 1 Schematic diagram of the experimental setup.

was used to control the ICCD camera parameters. The emission spectra display, processing and analysis were performed using 2D- and 3D-Gram/32 software programs (National Instruments, USA). In addition to the atomic database used by the mentioned software, spectral lines identification was checked against the most up-to-date electronically published database [15].

The gate width and delay time were chosen after performing systematic experimental optimisation of two important parameters. To optimise the signal-to-noise ratio and spectra reproducibility, the detection of spectra was carried out by averaging 10 single accumulations collected from 10 fresh target positions. The plasma emission spectra were collected under the effect of different values and polarities of electric field varying from 0 to 10 kV at atmospheric pressure. To ensure the reproducibility of the obtained results, the experiment was repeated several times.

The laser-induced shock waves (SWs) were probed following the method described in Azzeer et al. [16]. Using two corner tubes, a He–Ne laser beam was used to probe the propagating shock wave front at 3 consecutive positions as shown in Fig. 2(a). A fast photodiode was used to detect the deflection (refraction) of the probe beam at each intersection giving rise to a corresponding negative pulse of the oscilloscope trace as shown in Fig. 2(b). Knowing the distance between the two He–Ne beams and the corresponding time intervals between the CRO signals, the velocity of the propagating SW could be determined for the two successive time intervals.

Two polished parallel copper plates, 1.9 cm apart, were used as the electrodes for the application of the high voltage. The electrodes were both 60 mm diameter and 8 mm thick. One of the electrodes had a 5 mm diameter hole in its centre to permit focusing of the laser light on to the surface of the aluminium target impeded on the other electrode. Through the connection of the two electrodes with the high voltage (HV) power supply it was possible to reverse their polarity in order to study such effect. The target was a 5 mm polished high purity aluminium plate (99.9999%), with its surface facing the laser on the same level of the copper electrode surface to avoid any probable edge discharges. The target electrode holder

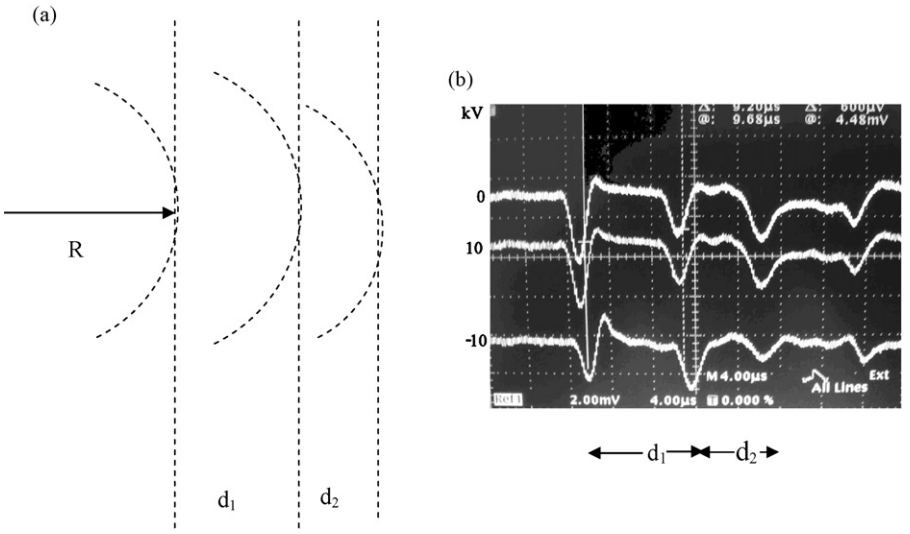

Figure 2 The propagating shock wave (SW) front at 3 consecutive positions (a); the corresponding negative pulses of the oscilloscope trace (b).

was fixed on a micro-translation stage facilitating fresh location for the laser focusing onto the Al surface.

Results and discussion

Optimisation of experimental parameters

For the spectral analysis of the laser-induced plasma, we followed the spectral lines evolution under different experimental conditions. The emission spectrum was recorded at different delay times (τ_d) and gate widths (Δ_t) in order to select the optimal signal-to-noise ratio (S/N) [17]. Here it must be noted that it was impossible to perform the measurements without delaying the measurement time with respect to the firing time of the laser as it was necessary to get rid of the overwhelming bright continuum at the early times of the plasma evolution [18]. Accordingly, in order to obtain a good S/N ratio, i.e. an optimum value of the emission intensity with respect to the background, a proper choice of the delay time was required for the measurement of both ionic and neutral spectral lines. To perform such optimisation, delay time was changed in the time interval between 50 ns to 5 μs at constant gate width (2.5 μs). The same procedure was performed to optimise the gate width at constant delay time (1.5 μs). Fig. 3 depicts the optimisation process of the delay time, revealing an optimum value $\tau_d = 1.5$ μs for both ionic and atomic emission lines. The obtained optimum values for Δ_t and τ_d were 2.5 and 1.5 μs respectively. It is worth mentioning here that both Δ_t and τ_d are functions of the other experimental parameters, such as the laser pulse energy, laser wavelength, and target characteristics. All these parameters were fixed throughout the experimental measurements to the values used during the optimisation of both Δ_t and τ_d.

Normalisation of the spectra to background

Normalisation of the maximum line intensities was exploited to avoid any unwanted experimental fluctuations by dividing each spectrum with their own background value.

The aluminium spectral lines used in the analysis throughout the present work were: 256.78, 266.5, 305.02, 309.3, 394.4 and 396.15 nm for atomic aluminium (Al I), and 281.64, 358.6 and 466.4 nm for ionic aluminium (Al II). Such lines and their physical parameters are listed in Table 1. The spectroscopic data were retrieved from Reader et al. [19].

Influence of electric field on the Al spectra

Fig. 4 shows a typical three-dimensional panoramic LIBS spectra of a pure Al target (99.999%) at 1.5 μs delay time and 2.5 μs gate width for different values of the applied electric field. The laser pulse energy was 60 mJ and the alignment of the optical fibre was such that it collected the light emission from the central part of the plasma plume. The figure reflects the wide spectral range and the high resolution furnished by the echelle spectroscopic system used. Data reproducibility can be enhanced through the accumulation of consecutive measured spectra. The spectra shown in Fig. 4 are the average of accumulating 10 single shot spectra. This figure also depicts the difference between the positive and negative biasing voltage cases. A careful investigation of the obtained spectra revealed that both the ionic and atomic spectral lines were affected (though differently) by the application of the electric field.

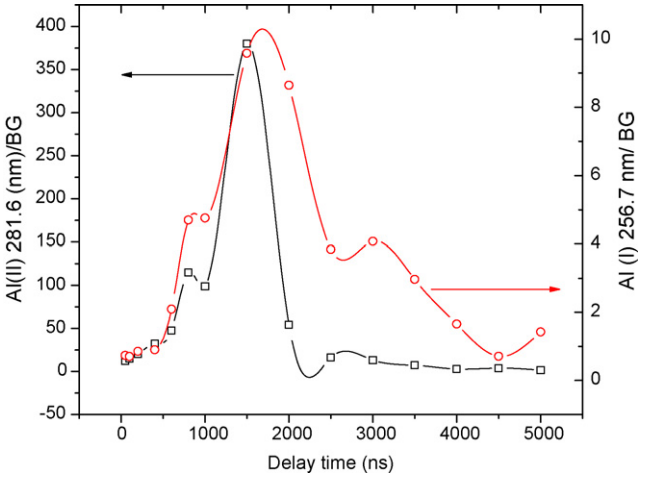

Figure 3 Optimisation of the delay time (τ_d) of the ionic lines and the atomic lines at constant gate width of 2.5 μs.

Table 1 Aluminium spectral emission atomic and ionic lines used in the present work and their physical parameters.

Species	λ (nm)	Configuration	Terms	$J_i - J_k$	A (s^{-1}) $\times 10^8$	E_i (cm^{-1})	E_k (cm^{-1})	g_i	g_k
Al	256.8	$3s^2 3p–3s^2(^1S)nd$	$^2P^\circ–y\ ^2D$	1/2–3/2	0.22	0.0	38,929	2	4
I	266.0	$3s^2 3p–3s^2 5s$	$^2P^\circ–^2S$	3/2–1/2	0.264	112	37,689	4	2
	305.0	$3s3p^2–3s3p(^3P^\circ)4s$	$4P–4P^\circ$	3/2–5/2	0.053	29,067	29,067	4	6
	308.2	$3s^2 3p–3s^2\ 3d$	$^2P^\circ–^2D$	1/2–3/2	0.61	0.0	32,435	2	4
	309.2	$3s^2 3p–3s^2\ 3d$	$^2P^\circ–^2D$	3/2–5/2	0.12	112	32,435	4	4
	394.4	$3s^2 3p–3s^2\ 4s$	$^2P^\circ–^2S$	1/2–1/2	0.493	0.0	25,348	2	2
	396.6	$3s^2 3p–3s^2\ 4s$	$^2P^\circ–^2S$	3/2–1/2	0.98	112	25,348	4	2
Al	281.6	$3s3p–3s\ (^2S)\ 4s$	$^1P^\circ–^1S$	1–0	3.83	59,850	95,348	3	1
II	358.6	3s3d–3s4f	$^3D–^3F^\circ$	3–4	2.45	95,549	123,423	7	9
	466.4	$3p^2–3s4p$	$^1D–^1p^\circ$	2–1	0.53	85,479	106,918	5	3

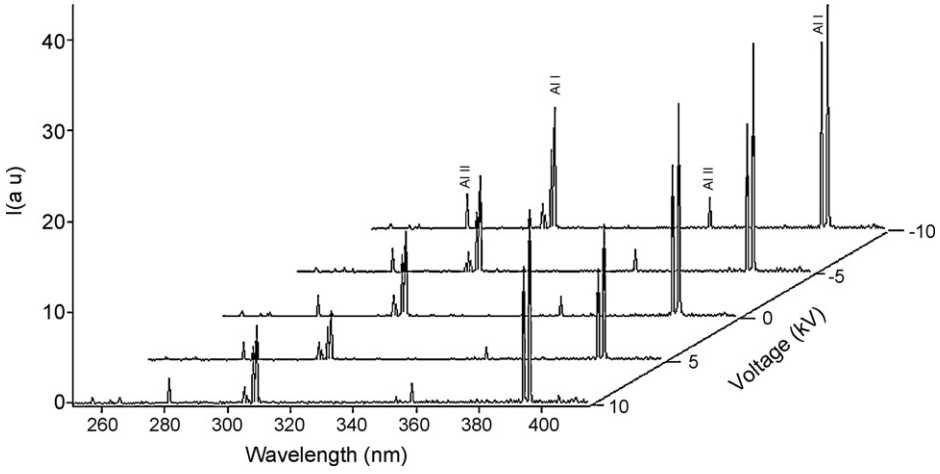

Figure 4 Typical 3D LIBS spectra of pure Al in the presence of a static electric field at various voltages. The laser pulse energy was 60 mJ, plasma emission was accumulated with a delay time 1.5 μs and gate width of 2.5 μs.

Influence of electric field on the Al II lines

As shown in the 3D map in Fig. 5, enhancement took place in the S/N ratio of ionic lines 281.63 as a consequence of the forward biasing of the electrodes, i.e. negative target and positive front electrode. Reversing the polarity resulted in a clear deterioration of S/N ratio.

The experimental points are plotted in the histogram shown in Fig. 6. This shows that a growth was obtained in the intensity (normalised to the background) of both aluminium ionic lines in the case of forward biasing. A doubling in the radiation intensity of the 281.63 nm spectral line was obtained at −10 kV biasing voltage compared with the zero voltage value. At reversed polarity, the line intensity deteriorated by 0.8 times at 10 kV with respect to the zero field value.

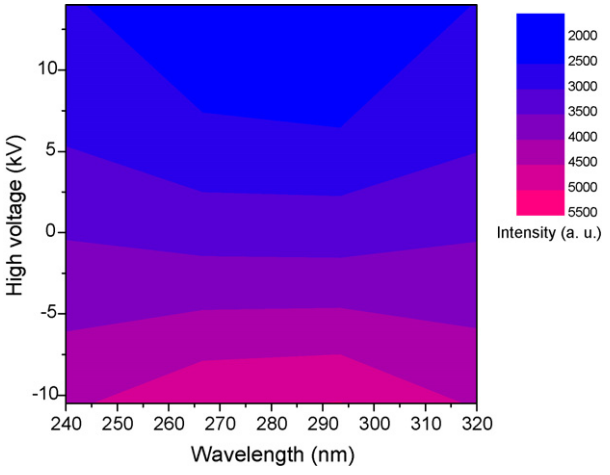

Figure 5 3D map for the influence of application of the high voltage with different polarities on the Al ionic spectral lines (281.64 nm).

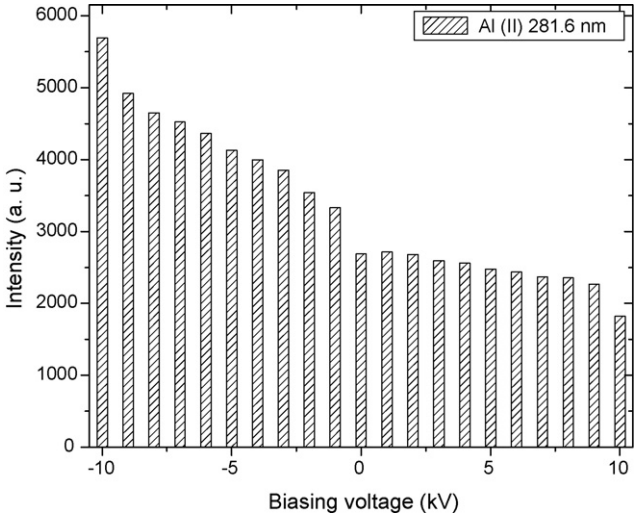

Figure 6 The biasing voltage dependence of the Al (281.63 nm) ionic line intensity normalised to the background.

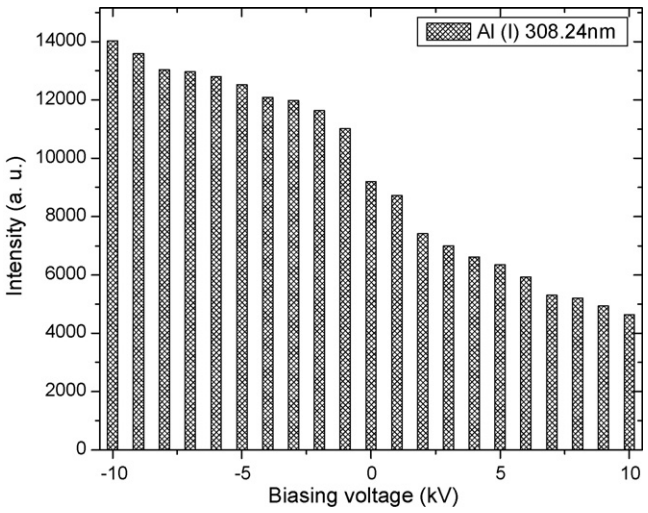

Figure 7 The biasing voltage dependence of the Al (308.2 nm) atomic line intensity normalised to the background.

The observed enhancement in the plasma emission ionic lines intensity in the UV and visible regions under forward biasing can be interpreted physically in view of the ionic nature of the plasma. It is well known that a laser-induced plasma plume moves in the direction opposite to the incident laser beam. The high repelling field between positive ions in the plasma and the positive front electrode leads to the confinement of the plasma plume. This increases the recombination probability, and consequently the emitted light intensity (radiative decay of excited atoms, ions or molecules). On the other hand, under reversed polarity (positive target), the deterioration in the plasma emission intensity occurs due to the high attractive field between the positive ions and the negative front electrode that leads to a decrease in the recombination rate due to the stretching of the plasma plume. Raising the voltage over 10 kV leads to a saturation effect, before the onset of the electric discharge in air at about 15 kV biasing voltage.

The influence of electric field on the Al I lines

Fig. 7 displays the effect of applying the electric field on the atomic lines at 308.2 nm. The same effect was pronounced in this case, since the emission originated from neutral atoms that are expected to have the response for the applied static electric field. Further, the increase in the intensities of the atomic line under forward biasing may be attributed to the reduction in self-absorption of such lines. The confinement of the plasma plume under the effect of the retarding electric field reduces the outer, colder, layer of the atoms responsible of self-absorption. In consequence, this may lead to the pronounced slight enhancement in the atomic lines intensities.

Plasma parameters

Plasma temperature

The emitted spectral line intensity I_{ki} is a measure of the population of the corresponding energy level of this element in the plasma, at local thermodynamic equilibrium (LTE). Accordingly, the population of an excited level can be related to the total density C_s of neutral atom or ion of the element through Boltzmann's law [7,20]

$$I_\lambda = F \cdot C_s \frac{A_{ki} g_k}{U_s(T_e)} \exp\left(-\frac{E_k}{kT_e}\right) \tag{1}$$

where A_{ki} is the transition probability, g_k is the statistical weight for the upper level, E_k is the excited level energy, T_e is the temperature, k is Boltzmann's constant, $U_s(T_e)$ is the partition function of the species and F is an experimental factor.

There are two main factors influencing the emitted line intensity. The first is the number density of the atoms and the second is the temperature of the plasma. Reformulating Eq. (1) gives

$$\ln \frac{I_\lambda}{A_{ki} g_k} = -\frac{1}{kT_e} \cdot E_k + \ln \frac{C_s F}{U_s(T_e)} \tag{2}$$

Measuring the relative line intensity it is then possible to estimate the plasma temperature T_e by plotting the left hand side of Eq. (2) vs. the excited energy level E_k. The plasma temperature can then be evaluated from the slope of obtained straight line.

According to these requirements the wavelengths of the atomic lines selected to determine plasma temperature were 257.57, 266.07, 309.32, 394.44, and 396.19 nm.

The required parameters in Boltzmann's method are listed in Table 1. Typical Boltzmann's plots of the aluminium lines are shown in Fig. 8(a–c), where the curved slopes yield the plasma temperatures. The aluminium plasma temperatures obtained as a function of the electric field with different polarities can be calculated from the slopes of the corresponding Boltzmann's plots.

As shown in Fig. 9, the plasma temperature tends to fluctuate slightly around a constant value with the increasing electric field in both directions. This effect may be due to the fact that the measured values of T_e are averaged over the whole plasma emission. More accurate values can be obtained by performing spatially resolved spectroscopic measurements.

Electron density

The electron density is an important parameter used to describe the plasma environment and is crucial for establishing its equilibrium status. The electron density can be estimated from the profile of the spectrum, which is a result of many effects, though mainly Stark broadening, Doppler broadening and pressure broadening effects. However, in the experimental conditions of the present work the main contribution to line widths arose from the Stark effect.

The profile for Stark broadened lines is well described by a Lorentz function. The well resolved Al (II) 281.6 nm spectral line was used to measure the full-width at half-maximum (FWHM). Since the instrumental line broadening exhibited a Lorentzian shape, the Stark line width $\Delta\lambda$ can be extracted from the measured line width $\Delta\lambda_{\text{obs.}}$ by subtracting the instrumental line broadening $\Delta\lambda_{\text{inst.}}$:

$$\Delta\lambda = \Delta\lambda_{\text{obs.}} - \Delta\lambda_{\text{inst.}} \tag{3}$$

In our case $\Delta\lambda_{\text{inst.}}$ was 0.05 nm (determined by measuring the FWHM of the Hg lines emitted by a standard low presser Hg lamp).

The width of the Stark broadened spectral line depends on the electron density (N_e). For the linear Stark effect the electron density and the line width are related by the simple formula

$$N_e = C(N_e, T_e)\, \Delta\lambda^{3/2} \tag{4}$$

where the parameter $C(N_e, T_e)$ determines the relative contribution of the electron collision on the electrostatic fields, depending weakly on N_e and T_e.

For a non-H like line, the electron density (in cm^{-3}) can be determined from the line width as:

$$N_e \approx \left[\frac{\Delta\lambda}{2w}\right] \cdot 10^{16} \tag{5}$$

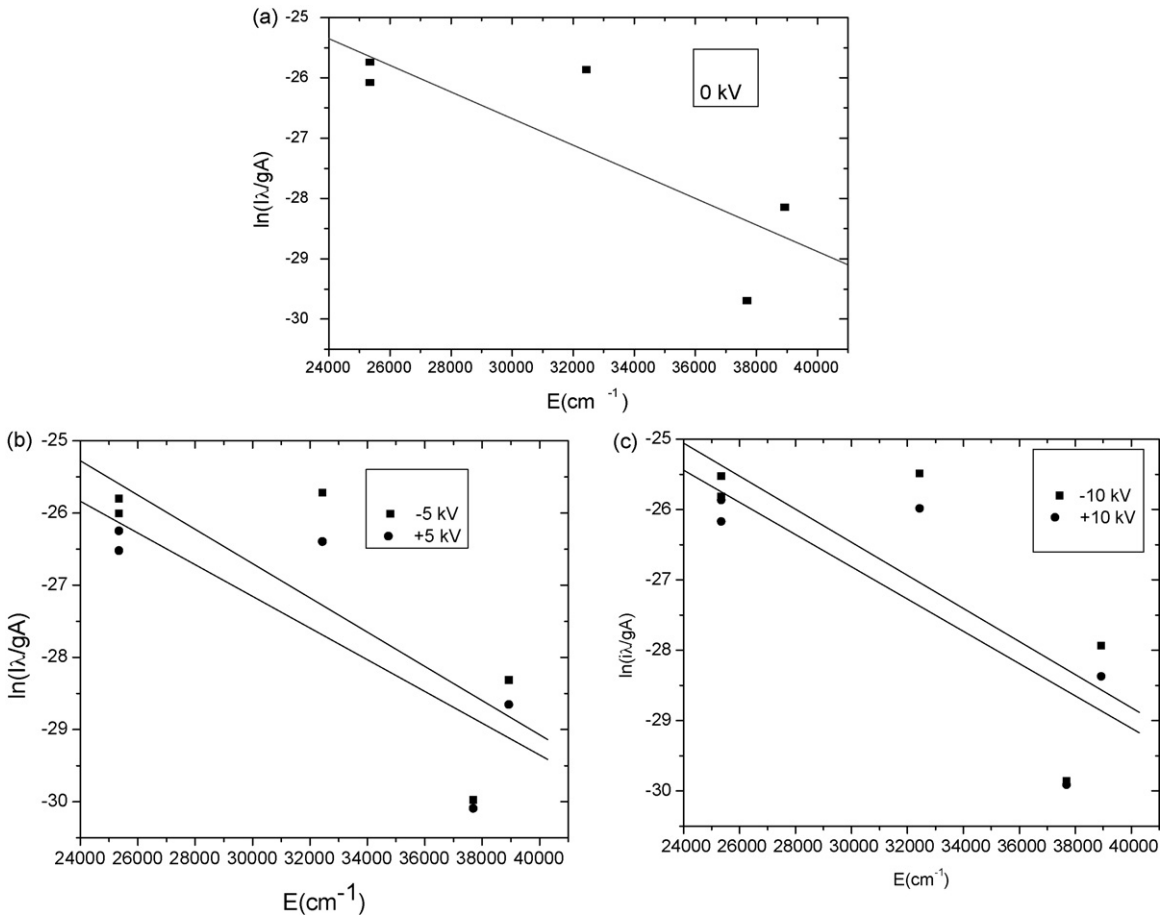

Figure 8 (a–c) Boltzmann's plots for Al I spectral lines at different high voltages and polarities.

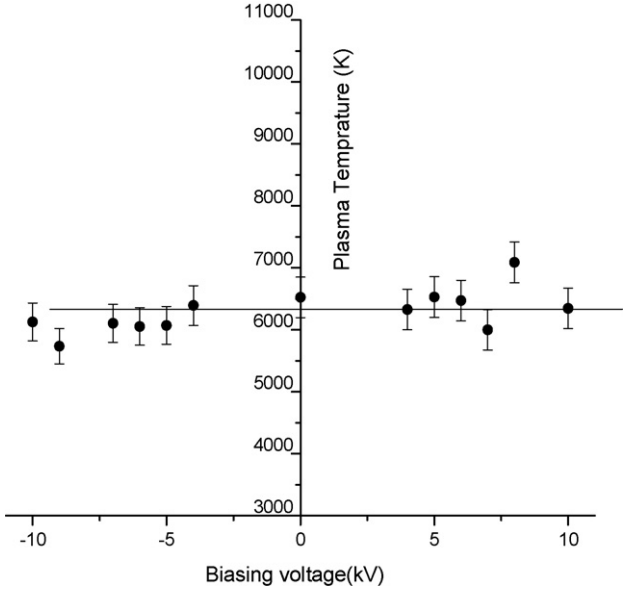

Figure 9 Applied voltage dependence of the plasma temperature measured spectroscopically using Boltzmann's method. The error bars represent the experimental data standard deviation.

The parameter w is the electron impact value, which can be found in the well-documented table [21].

As shown in Fig. 10 no significant effect was observed in the electron density in the case of reverse biasing. This may be due to the fact that the high voltage had no effect on the line broadening.

Local thermodynamic equilibrium

By knowing the electron density and the plasma temperature we can determine whether the local thermodynamic equilibrium (LTE) assumption is valid by applying McWhirter criterion [22]. The lower limit for the electron density at which the plasma will be in LTE is given by [9,20]:

$$N_e(\mathrm{cm}^{-3}) \geq 1.6 \times 10^{12}[T_e(K)]^{1/2}[\Delta E(eV)]^3 \quad (6)$$

ΔE is the largest energy transition for which the condition holds and T_e is the excitation temperature.

In the present case $\Delta E = 3.65$ eV. The electron density lower limit value given by Eq. (5) for aluminium plasma is 6.9×10^{15} cm^{-3}. The experimentally calculated densities were greater than these values, consistent with the assumption that the LTE is prevailing in the plasma.

Effect of high tension on shock wave (SW) propagation

The propagation of the shock wave front causes the He–Ne laser beam to deflect (refract) at each intersection—giving rise to a cor-

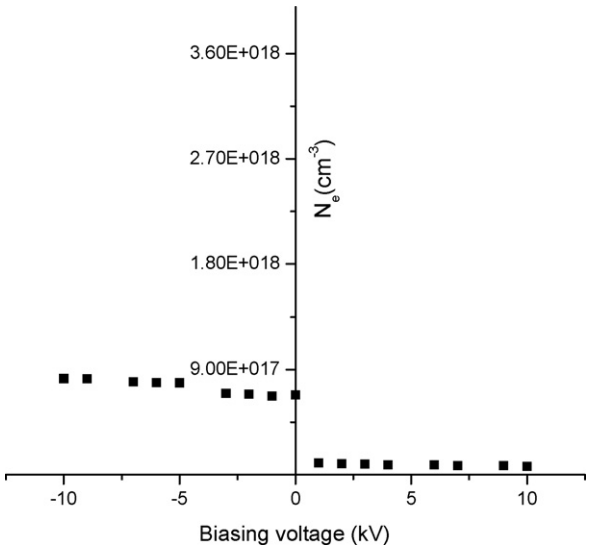

Figure 10 Applied voltage dependence of the electron density (obtained using Al II at 281.6 nm).

responding negative pulse of the oscilloscope trace (see Fig. 2). Since the He–Ne beams were separated with well known distances $d_1 = 11$ mm and $d_2 = 4$ mm and as the time intervals between the corresponding oscilloscope signals were known, we can determine the velocities u_1 and u_2 of the propagating shock wave at two successive time intervals. In this way the shock wave velocity was calculated under the effect of different high-tension strengths and at different polarities. The results show that there is no significant influence of the high tension on the shock wave velocity. The obtained average values of u_1 and u_2 were 4.5 and 2 Mach respectively. However, the values of the SW velocity may be used to monitor the stability of the laser-produced plasma and can also be used to normalise the obtained spectra [23].

Conclusion

In the present work laser induced breakdown spectroscopy was applied to a pure aluminium target impeded in one of two copper electrodes in order to investigate the effect of electric field on the LIBS signal. We also studied the influence of an electric field on the plasma parameters produced on the pure aluminium target as well as laser-induced shock waves.

The results show that the electric field had a pronounced effect on the emission intensities of the ionic lines under forward biasing (negative target). In general, the emission of the ionic lines grew exponentially. In the reversed biasing case, the line intensity deteriorated with respect to the zero field value. The effect on atomic lines was not clear, with no real change noticed under forward biasing.

As for the effect of applying the electric field on the plasma parameters, the plasma temperature tended to fluctuate slightly around an average constant value with the increasing electric field in both directions. On the other hand the electron number density was found to decrease slightly in the case of forward biasing, with a much stronger decrease (about one order of magnitude) in the case of reversed biasing.

As expected, no electric field effect was noticed on the laser-induced shock wave velocity. In fact, the SW velocity depended mainly on the laser parameters, such as pulse energy and spot size.

It has been shown that the application of the static electric field on the LIP in the forward direction improves the signal-to-noise (S/N) ratio of the LIBS signals. Accordingly, it is feasible to improve the limit of detection (LOD) of the LIBS technique adopting this method. The results of the present study can be utilised in order to improve LIBS application in industrial production control.

References

[1] Goode SR, Morgan SL, Hoskins R, Oxsher A. Identifying alloys by laser-induced breakdown spectroscopy with a time-resolved high resolution echelle spectrometer. J Anal Atom Spectrom 2000;15(9): 1133–8.
[2] Charfi B, Harith MA. Panoramic laser-induced breakdown spectrometry of water. Spectrochim Acta B 2002;57(7):1141–53.
[3] Nordstrom RJ. Study of laser-induced plasma emission spectra of N_2, O_2 and ambient air in the region 350 nm to 950 nm. Appl Spectrosc 1995;49:1490–9.
[4] Cremers DA, Radziemski LJ. Handbook of Laser-induced Breakdown Spectroscopy. Wiley; 2006.
[5] Miziolek WA, Palleschi V, Schechter I. Laser Induced Breakdown Spectroscopy (LIBS): Fundamentals and Applications. Cambridge, UK: Cambridge University Press; 2006.
[6] Barbini R, Colao F, Fantoni R, Palucci A, Capitelli F. Laser induced breakdown spectroscopy for quantitative elemental analysis. Proc SPIE 2000;4070:444–9.
[7] Elhassan A, Giakoumaki A, Anglos D, Ingo G, Robbiola L, Harith MA. Nanosecond and femtosecond laser induced breakdown spectroscopic analysis of bronze alloys. Spectrochim Acta B 2008;63(4): 504–11.
[8] Abdel-Salam ZA, Galmed AH, Tognoni E, Harith MA. Estimation of calcified tissues hardness via calcium and magnesium ionic to atomic line intensity ratio in laser induced breakdown spectra. Spectrochim Acta B 2007;62(12):1343–7.
[9] Galmed AH, Harith MA. Temporal follow up of the LTE conditions in aluminum laser induced plasma at different laser energies. Appl Phys B 2008;91(3–4):651–60.
[10] St Onge L, Sabsabi M, Cielo P. Analysis of solids using laser-induced plasma spectroscopy in double-pulse mode. Spectrochim Acta B 1998;53(3):407–15.
[11] Amal K, El Naby SH, Palleschi V, Salvetti A, Harith MA. Comparison between single- and double-pulse LIBS at different air pressures on silicon target. Appl Phys B 2006;83(4):651–7.
[12] Aguilera JA, Aragón C. A comparison of the temperatures and electron densities of laser-produced plasmas obtained in air, argon and helium at atmospheric pressure. Appl Phys A 1999;69(7): S475–8.
[13] Rai VN, Rai AK, Yueh FY, Singh JP. Optical emission from laser-induced breakdown plasma of solid and liquid samples in the presence of a magnetic field. Appl Optics 2003;42(12): 2085–93.
[14] Hontzopoulos E, Charalambidis D, Fotakis C, Farkas G, Horváth ZG, Tóth C. Enhancement of ultraviolet laser plasma emission produced in a strong static electric field. Optics Commun 1988;67(2): 124–8.
[15] NIST electronic database. http://physics.nist.gov/PhysRefData.
[16] Azzeer AM, Al Dwayyan AS, Al Salhi MS, Kamal AM, Harith MA. Optical probing of laser-induced shock waves in air. Appl Phys B 1997;63(3):307–10.
[17] Body D, Chadwick BL. Optimization of the spectral data processing in a LIBS simultaneous elemental analysis system. Spectrochim Acta B 2001;56(6):725–36.
[18] Hermann J, Vivien C, Carricato AP, Boulmer Leborgne C. A spectroscopic study of laser ablation plasmas from Ti, Al and C targets. Appl Surf Sci 1998;127–129:645–9.
[19] Reader J, Corliss CH, Wiese WL, Martin GA. Wavelength and Transition Probabilities for Atoms and Atomic Ions. Washington, DC: U.S.

Department of Commerce, National Institute of Standards and Technology; 1980.
[20] Colao F, Lazic V, Fantoni R, Pershin S. A comparison of single and double pulse laser-induced breakdown spectroscopy of aluminum samples. Spectrochim Acta B 2002;57(7):1167–79.
[21] Griem HR. Plasma Spectroscopy. New York: McGraw-Hill; 1964.
[22] Lochte Holtgreven W. Plasma Diagnostics. Woodbury, NY: American Institute of Physics; 1995.
[23] Aragón C, Bengoechea J, Aguilera JA. Influence of the optical depth on spectral line emission from laser-induced plasmas. Spectrochim Acta B 2001;56(6):619–28.